Design and Experimental Evaluation of a BLDC Motor–Magnetic Gear Drive for a Rotating Biological Contactor

Alexandre Lebel[1*]

[1]Institute of Science and Environment, University of Saint Joseph, Macau, China
Email: alexandre.lebel@usj.edu.mo
[*]Corresponding author

Manuscript received February 26, 2026; revised Month date, 2023; accepted Month date, 2023

***Abstract*—Rotating biological contactors (RBCs) are recognized for their small footprint, reliability, and low energy demand. RBCs are a potential option for compact decentralized wastewater treatment systems, but pose scalability challenges and mechanical constraints. We present, as a proof-of-concept, design modifications to the RBC drive system that use an inner-rotor brushless direct current (BLDC) motor and a waterproof magnetic gearbox (MG) to drive rotating disks at low speeds (<1 rpm) while isolating electrical components from water. We assess 1) the magnetic air gap inside the sealed rim of the rotor, which can impair efficient torque transfer, and 2) the maximum output torque of the MG limited by the strength of the magnets and the air gap flux. Our results show that the BLDC's performance is adequate even with a large radial air gap, but the electronic overhead significantly reduces overall efficiency in a small system. Also, the MG's torque capacity is sufficient to maintain the system's rotation.**

***Keywords*— BLDC, magnetic gearbox, rotating biological contactor, wastewater, decentralized WWTP**

I. Introduction

The complexity of advanced wastewater treatment technology, combined with high investment and operational costs (including skilled personnel and energy requirements), often prevents the implementation of decentralized infrastructures [1]. Nevertheless, bioremediation strategies offer cost-effective, adaptable methods for removing specific contaminants and reducing their environmental and health impacts [2][3]. While decentralized wastewater treatment systems (DEWATS) emphasize the spatial distribution of infrastructure across a network, which can reduce energy use for collection and transport, they can also enhance treatment efficiency by allowing systems to be customized to specific pollutant types [4][5].

Regarding bioremediation strategies, rotating biological contactor (RBC) systems are widely recognized for their simple design, small footprint, reliability, and low energy consumption [6][7][8][9]. RBCs are biofilm-based wastewater treatment systems that use a series of rotating discs to support microbial growth. Biomass grows as a biofilm attached to the surface of the support media. While RBCs are a potential option for DEWATS, scalability issues and mechanical deficiencies limit their use [10][11]. Optimization of the motor drive assembly has been limited, especially given recent advancements in mechanical engineering. In this paper, we demonstrate, as a proof-of-concept, design modifications to RBCs to mitigate mechanical stress and direct water ingress to the drive assembly. We explore the feasibility of using an inner-rotor BLDC motor and a waterproof magnetic gearbox to drive rotating disks at low speeds while isolating electrical components from water.

II. Literature Review

The RBC rotation drive typically employs a three-phase induction motor, gearbox, drive shaft, and bearings. The drive must handle high torque at low speed, resist corrosion, run continuously, and be easy to maintain. Industrial-grade induction motors (3.7-5.6 kW) can operate continuously for years, with maintenance intervals ranging from 5,000 to 20,000 hours [12]. However, induction motors require a constant magnetizing current, which prevents scaling down. Consequently, a gear reducer achieves a low rotational speed, and the motion is transmitted to the discs via a chain-and-sprocket or V-belt drive, which requires additional maintenance [13]. In comparison, BLDCs use permanent magnets and electronic commutation rather than brushes and a physical commutator, thereby reducing mechanical wear from sliding contact. Moreover, BLDCs can be designed to operate directly at low speeds without a gearbox [14][15]. Field-oriented control (FOC) regulates torque and speed via current control, allowing the drive to adapt its torque output to load demand. As a result, only the current required to maintain the commanded operating rotation speed is supplied, reducing energy consumption [16][17]. BLDCs can potentially achieve higher efficiencies than traditional induction motors, due to the elimination of gearbox losses and inefficiencies associated with low-speed operation.

Many RBC systems were implemented during the 1970s and 80s, when BLDCs were not affordable due to the costs of complex electronics and rare-earth permanent magnets. For instance, since the early 1980s, neodymium-iron-boron (NdFeB) permanent magnets have become technologically superior to other materials, and improvements in manufacturing have significantly reduced their cost over the past four decades [18]. Additionally, since the 2000s, low-cost control technologies (affordable single-chip integrated controllers and sensorless control schemes) have spurred the adoption of BLDCs across various industrial applications [19][20]. Although BLDC motors can operate at low speeds, a gearbox may be necessary to meet the RBC system's rotation requirements, typically below 10 rpm [21][22]. Yet, the introduction of NdFeB permanent magnets enabled the development of magnetic gearboxes (MGs), which achieve speed reduction and torque multiplication while eliminating physical contact between moving components, resulting in lower friction and minimal maintenance compared to conventional mechanical gears [15][23].

Despite their design and operational simplicity, RBC systems are subjected to mechanical stress and exposure to the elements [10]. The corrosion of support structures and improper maintenance of moving parts (shafts and bearings) can lead to mechanical failures [13][24]. In that regard, BLDC technology is notably beneficial for marine propulsion, especially in rim-driven thruster designs, where the motor is enclosed in a watertight housing without a shaft seal [25]. Similarly, MGs are inherently suited for submerged applications due to their ability to provide non-contact torque transmission. Combining BLDC and MG eliminates the leak paths typically associated with dynamic shaft seals.

In Fig. 1, we compare design choices for the RBC drive assembly presented in this study. For low-speed, high-torque operation, BLDC motors operated under FOC offer improved efficiency and torque controllability compared to induction motors. An in-runner BLDC motor is preferred for submerged applications due to its enclosed rotor geometry, which simplifies sealing and mitigates corrosion. Although sensored FOC is well-suited for low-speed applications, sensorless FOC reduces hardware complexity, which is preferable for harsh environments. MGs have lower torque density than traditional mechanical gearboxes, but offer contactless operation, intrinsic overload protection, and reduced maintenance. Similarly, an axial-flux MG design offers lower torque density than other MG configurations, but its flat assembly is suitable for modular stacking, thereby increasing the transmission ratio in a compact system.

Two main elements in the selected design must be assessed: 1) the magnetic air gap inside the sealed rim of the rotor can impair efficient torque transfer, and 2) the maximum output torque of MGs is limited by the strength of the magnets and the air gap flux. Ultimately, the output torque of the final stage of a cascaded MG limits the load, regardless of the motor input. Nevertheless, we argue that in wastewater treatment processes, these implementations can directly address challenges related to size, maintenance, energy consumption, and water ingress, making RBC systems suitable for compact DEWATS.

III. Materials and Methods

1) BLDC customization

Evaluation experiments used a custom inner-rotor BLDC (Fig. 2) with a stator winding of 18 slots (ID 160 mm, 0.9 mm enamel-coated copper wire, 80 turns per slot, and Y-configuration) and a lightweight 3D-printed PETG rotor with 20 poles (OD 156 mm). Each rotor pole contained a grade N52 NdFeB permanent magnet (20 × 20 × 3 mm each, measured pole flux density ≃ 250 mT) and an iron backing (3 mm silicon steel laminations). A 3D-printed PETG pipe adaptor (OD 160) was inserted inside the stator, such that electrical parts were isolated. A 2 mm radial air gap between the stator and rotor corresponds to the thickness of the PETG adaptor (1 mm) plus the minimal space required for the rotor to spin freely (1 mm).

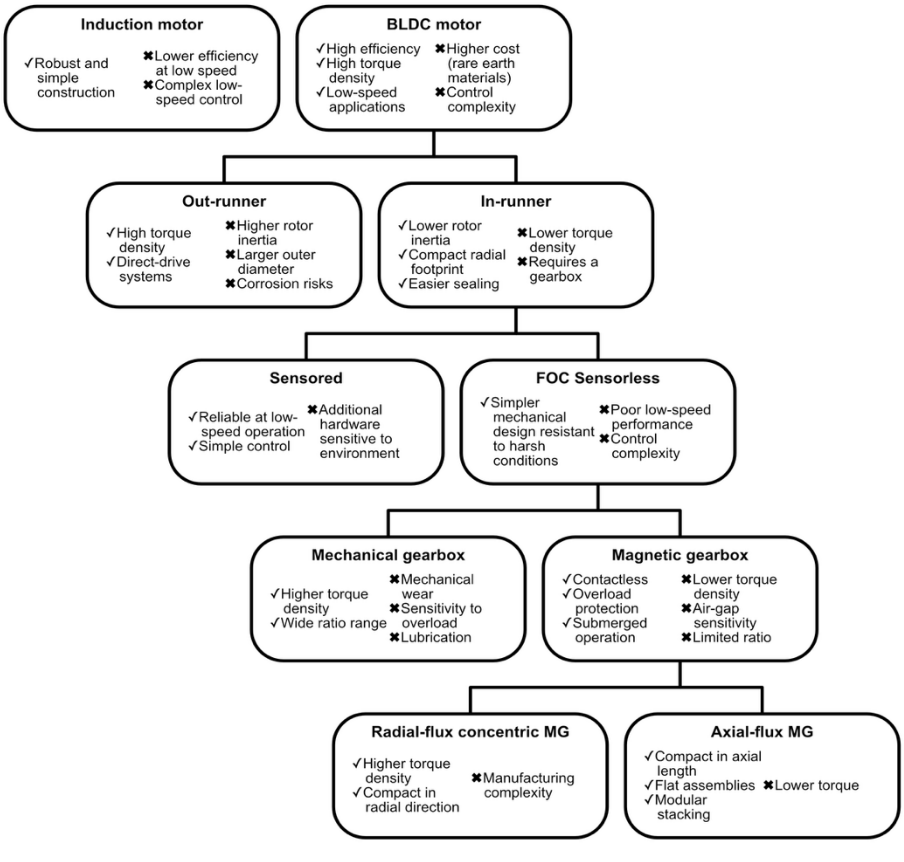

Fig. 1. The figure illustrates the design decision tree, highlighting the key components of RBC drive assemblies. The selected options are shown on the right-hand branches.

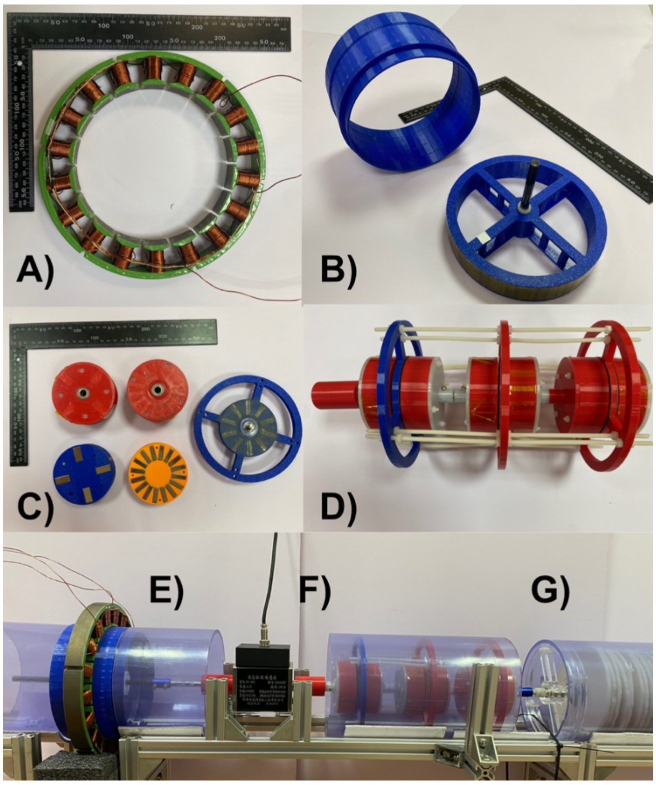

Fig. 2. The 18-slot in-runner stator (A) is isolated from the 20-pole rotor using a PETG pipe adaptor (B). In C), the MG examples consist of a 4-pole fast rotor, 16-pole slow rotor, and 10-pole stationary modulator. Three identical MGs in cascade produced a 64:1 reduction ratio (D). The rotor hub is secured to the shaft with a set screw and supported by ceramic bearings in an acrylic housing within the pipe adaptor (E). An inline rotating torque meter (F) measures the mechanical power transmitted between the motor and the load (MG and RBC module) (G).

2) BLDC Control

The LAUNCHXL-F28069M LaunchPad development kit (Texas Instruments) used the TMS320F28069M microcontroller unit (MCU) to control the BOOSTXL-DRV8301, a 3-phase brushless gate-driver and power stage module. The motor's control algorithms, parameter identification routines, and parameter estimation functions were implemented using the TI MotorWare™ software development kit, and the InstaSPIN-FOC™ framework [26]. The code was customized and compiled using TI Code Composer Studio™ IDE (Ver. 20.4.0). The code implementation and motor configuration were developed using the InstaSPIN™ Universal GUI.

3) Magnetic gearbox

The BLDC was coupled to a magnetic gearbox to reduce rotational speed. The 3D-printed gearbox used a PETG housing (⌀ 80 mm), permanent magnets (N52 NdFeB), and ferromagnetic laminations (silicon iron). The magnetic gearbox comprises three main components: a low-speed rotor with 8 pole pairs (3 stacked magnets per pole, 10 x 6 x 6 mm each), a stationary flux modulator with 12 ferromagnetic segments (10 x 6 x 6 mm each), and a high-speed rotor with 4 pole pairs (2 stacked magnets per pole, 20 x 10 x 10 mm each). The low-speed and high-speed rotors used segmented silicon-iron backings (thickness = 5 mm) to provide a low-reluctance return path for the magnetic flux. Ceramic bearings supported the gearbox's rotor components. ABS spacers maintained the air-gap (1 mm) between the rotor magnets and modulator, ensuring efficient magnetic flux transmission. Three identical magnetic gear stages, each with a 4:1 reduction ratio, were cascaded to achieve an overall transmission ratio of 64:1.

4) Biological Rotating Contactors

The RBC consisted of modular sections containing 36 wool felt discs (⌀ 130 mm, thickness = 5 mm, spacing = 5 mm) mounted on a nylon shaft (500 mm). The shaft was supported at multiple locations using intermediate ceramic bearings to maintain alignment. The total supporting media area was approximately 0.475 m^2, corresponding to a theoretical volume of approximately 4.4 L at 50% submergence, including running clearance. The effect of wet operation on hydrodynamic drag torque was approximated by using the MG's maximum torque as a limiting factor. Although the intended application involves submerged operation, the motor and drivetrain assembly was tested in dry conditions, isolated from the RBC unit, to allow mechanical and electrical measurements.

5) BLDC Evaluation

The drive prototype was operated under suboptimal conditions to demonstrate feasibility rather than optimized performance. The test bench for evaluating the motor's electrical and mechanical parameters and control behavior integrated test and measurement instrumentation: programmable power source (Siglent SPD1305X-C: ±0.01V, ±0.01A); digital power meter (Uni-T UTE9802+: ±0.001V, ±0.001A); oscilloscope (Siglent SDS1104X-C: 100 MHz, 1 GSa/s, 8-bit), current probe (Hantek CC-65: DC-20kHz, 100mV/A, ±2%); differential voltage probe (Hantek HT8100: 500:1, 100 MHz, ±2%); tachometer (Uni-T, UT372, ±0.04%+2); gaussmeter (Uni-T UT335C: ±0.1; incremental quadrature encoder (YunYu JYP38/8-360BZ-AT2J2, 5V TTL, 720 counts/ revolution); stall torque transducer coupled to a digital torque analyzer (ShenCe HP-50: 5 N·m, ±0.5%); in-line rotary torque transducer (JNSensor JN-DN5: 10 N·m, ±0.3%) coupled to a digital torque analyzer (JNSensor MCK-DN: ±0.2FS); %); magnetic powder brake (PFDE FZ-D-0.6KG-9-DZ: 6 N·m, 24V, 0.8A).

Electrical parameters, including stator resistance, inductance, and permanent-magnet flux linkage, were identified using the InstaSPIN-FOC™ motor identification routine with the motor uncoupled from the magnetic gearbox. The identified parameters were retained for torque and speed control for all closed-loop control experiments. The no-load back-electromotive force (EMF) was measured by manually spinning the rotor with a controllable DC motor and recording the induced voltage across the stator windings. We characterized the load- and speed-dependent efficiency behavior of the BLDC system. The gearbox's mechanical parameters were measured to confirm the transmission ratio and output torque, and the air-gap flux density was experimentally measured.

IV. Result and Discussion

1) General BLDC Parameters

We evaluated the magnetic coupling across the 2 mm radial air gap. We measured the motor's peak-to-peak voltage (V_{pp}) across two phases (line-to-line) without load, at different speeds (Fig. 3). The back-EMF constant is calculated from the measured slope (0.1264 V/rpm) under sinusoidal control, corresponding to a peak voltage (V_{pk}) of 0.0632 V/rpm (half of V_{pp} and equivalent torque constant k_t of 0.6035 N·m/A after converting rpm to rad/s). A low back-EMF constant can induce current ripple at low speeds, but in our system, a linear V_{pp} is consistent with expectations for FOC control. The electrical frequency (f_e) is linearly proportional to the mechanical speed (ω_m), thus confirming synchronous operation. Additionally, a stator winding resistance and inductance test was performed using the InstaSPIN-FOC™ motor identification routine. Phase resistance was measured using the DC current injection method, assuming a Y-connected winding. The results are presented in Table 1.

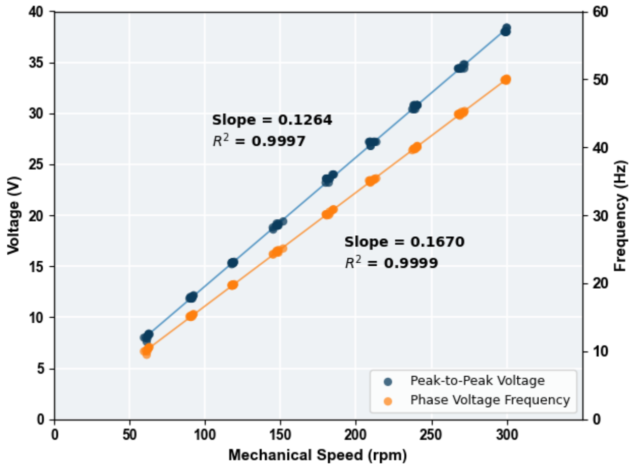

Fig. 3. Back-EMF peak-to-peak voltage (A-B) measured under no-load conditions at various mechanical speeds, showing a linear relationship with electrical phase frequency.

Table 1. General design parameters and electrical parameters, as measured using the InstaSPIN-FOC™ motor identification routine

Parameter	Value
Rs (Stator Resistance)	0.5705274 Ohms
Ld and Lq (D- and Q-axis Inductances)	4.7697382 mH
Flux Linkage (Ψ or Flux)	0.2338249 V/Hz
Pole Pairs	10 pairs
Back-EMF constant (k_e)	0.0632 V/rpm
Torque constant (k_t)	0.6035 N·m/A
DC bus voltage	24.00 V
Phase resistance (line-to-line) at room temperature	0.64 Ω
Speed range (min–max with stable RPM)	20-300 RPM

2) BLDC Performance

We characterized the load- and speed-dependent efficiency behavior of the BLDC system. First, we operated the motor at a fixed speed while gradually increasing the mechanical load (Fig. 4A); second, we operated at a constant load while adjusting the speed (Fig. 4B-C). The overall motor efficiency was defined as the ratio of mechanical output to electrical input power. The electromagnetic torque efficiency was defined as the ratio of mechanical output to electromagnetic torque (estimated as the product of k_t and the phase current root-mean-square I_{rms}). The electronic overhead (MCU and gate drivers) consumed 1.6 W. The input torque of the MG was near zero-load (0.05 N·m). By subtracting the baseline electronic consumption from the total input power, we isolated the motor's electromechanical conversion efficiency. Low efficiency at lower speeds and near-zero load (η ≈ 10-20%) reflects rotor inertia –high inertia is inherent to the large rotor diameter– and baseline losses, with the electronic overhead accounting for more than 50% of energy consumption. At higher speeds and with increasing torque, the electromechanical conversion efficiency reaches 60%, confirming that the design is adequate despite non-linearities at lower speeds and loads. Electromagnetic torque efficiency predictably decreases with speed, indicating parasitic losses (iron losses, eddy currents, friction). While those losses represent a smaller percentage at higher loads, we observe values above 100%, indicating that the linear k_t no-load estimation is insufficient to predict torque production, as it does not account for the reluctance torque due to rotor saliency, inherent to in-runner geometry. The difference between the electromagnetic torque and electromechanical conversion is mainly driven by the 2 mm radial airgap, which significantly increases magnetic reluctance.

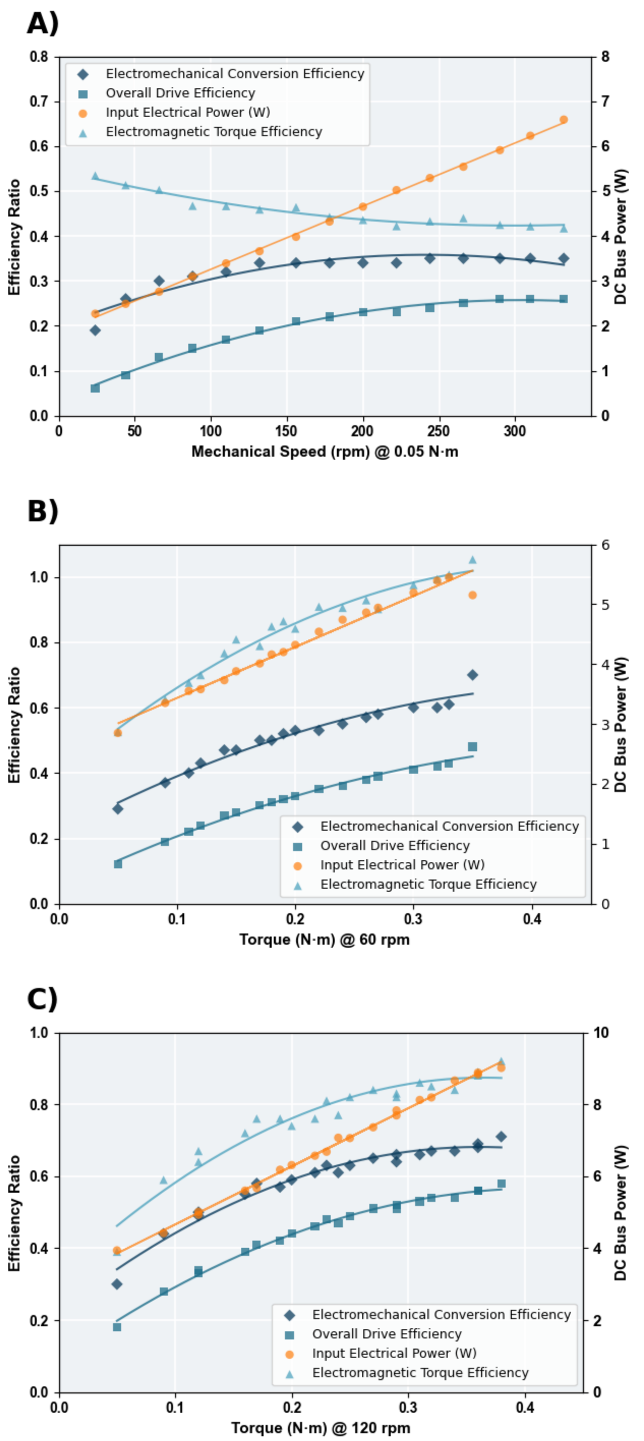

Fig. 4. Electrical input power (W) and efficiency behavior (%) of the BLDC at fixed load (0.05 N·m) and fixed speed (60 and 120 rpm). Electromechanical conversion efficiency accounts for the electronic overhead (1.6 W in idle state). The fixed load represents the input torque of the magnetic gearbox without the output load. The fixed speeds represent the intended operating range (1-2 rpm, accounting for the gearbox reduction).

The air gap is the largest magnetic reluctance in the motor's magnetic circuit, which may result in a lower back-EMF and lower torque output for the same current. Small- or medium-sized BLDC motors typically have an air gap of less than 1 mm. However, even with a 2 mm air gap, the BLDC drive performance is comparable to that of standard RBC systems, whose efficiency can range from 40 to 60%, when using high-ratio gear drives, such as worm gearboxes [27], and oversized motors for starting torque, but running at low loads during operation, resulting in sharp efficiency drops [28]. In comparison, in fisheries, BLDC-driven paddle-wheel aerators consumed 50% less energy than AC induction motors [29]. In fact, our results show that electromechanical conversion efficiency is adequate, although overall efficiency is significantly affected by baseline consumption (electronic drive) at such a small scale.

3) Magnetic gearbox

In this drive assembly design, the torque output at the load is primarily limited by the MG's effective torque transmission (i.e., maximum load before the MG slips). The actual gearbox transmission ratio, determined at various speeds, indicated that slipping was negligible compared to a theoretical 1:64 (Fig. 5).

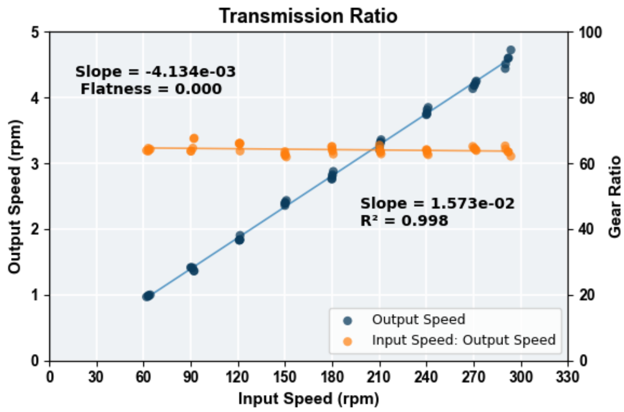

Fig. 5. Transmission ratio of the magnetic gearbox as the ratio between the input and output speed.

The MG's torque transfer efficiency depends on the change in flux linkage with the relative angle. We measured the flux density as a function of the angle around the face of the low-speed and high-speed rotors, through the modulator. In Fig. 6A, the sine-like wave of the slow rotor and the absence of a 'plateau' suggest that the modulator teeth are operating below saturation [30]. In Fig. 6B, the mountain-like waveform of the fast rotor shows that the flux rises gradually as a pole approaches the measurement point, peaks sharply when aligned, and then decreases. These irregularities in the flux plot may result in torque ripple at the output. However, torque and current ripples are not a concern for RBC applications, as the primary performance metric is oxygen transfer over extended operation rather than smooth, steady rotation.

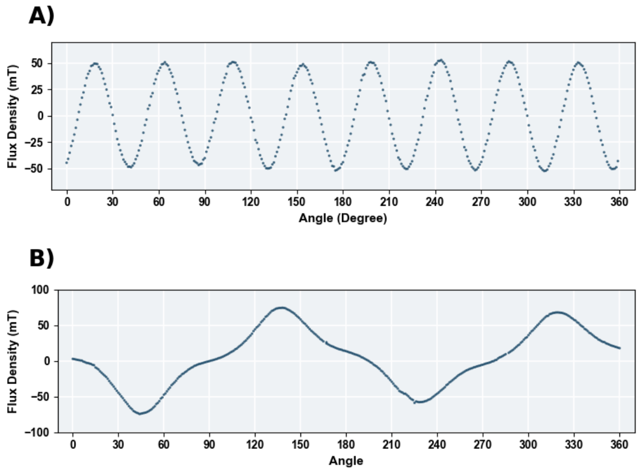

Fig. 6. Variation of flux density in airgap adjacent to low-speed (A) and high-speed rotors (B).

Further design optimization would increase operational performance. For example, the MG's rectangular magnets cover only 40% of the slow rotor and 16% of the fast rotor, resulting in 'dead zones' where no torque is transmitted. Using arc-shaped magnets would increase the total interaction area between the rotors. Moreover, magnetic gearboxes are highly sensitive to alignment, and specialized machining processes and precise positioning can greatly improve torque output. We should note that permanent magnets are susceptible to demagnetization due to heat, opposing magnetic fields, or mechanical stress. However, at low speeds (below 100 RPM), the risk for demagnetization is low: low back-EMF, low current stress, no high-speed heating.

4) Rotating biological contactor system

The maximum transmissible torque of the system (static slip torque = 0.8 N·m) occurs at the point at which the magnetic gear rotor begins to slip under increasing load, as measured with a reaction torque meter. The hydrodynamic drag torque was experimentally characterized using a single RBC module operated in water. The module could be driven at 70 rpm with 50% submergence, without noticeable slip (single MG with a stable 4:1 transmission ratio and torque load of 0.15 N·m). Since hydrodynamic drag decreases at lower rotational speeds, we estimated the maximum number of identical modules that could theoretically be driven at 1 rpm, assuming a viscous regime (drag exponent $n = 1$), negligible hydrodynamic interactions, and a slip speed of 70 rpm.

$$N_{max} = \left(\frac{\omega_{slip}}{\omega_{low}}\right)^n = \left(\frac{70}{1}\right)^1 = 70 \quad (1)$$

The scaling ratio does not account for the internal friction in the system. The actual limit is expected to be governed by bearing friction and low-speed drivetrain mechanical losses rather than fluid drag, given the longer rotating shaft. Additionally, the rotor and MG were not submerged during testing.

Wool felt was used as a realistic support medium [31], as it increases the hydrodynamic drag due to its high surface roughness and porosity. Our study demonstrates stable operation, suggesting that scalability and operation with lower-drag materials are feasible, although different materials may present their own practical challenges. Using a conservative derating factor of 10%, we estimate that, with proper alignment, a system could contain 7 modules, representing a total volume of 30 L. Despite a low transmission ratio and torque capacity, the MG is suitable for driving the RBC, as the BLDC motor can be operated directly at low rotational speeds, and the required load torque is modest (0.15 N·m and 70 rpm rotor output for an electrical input of 3 W). Considering the reported performance and removal efficiency of RBCs –a 4-hour hydraulic retention time can achieve over 80-90% removal of organic contents [32]– such a design could treat 180 L per day using 72 Wh/day, for a specific energy consumption of 0.4 kWh/m³.

Despite the inherent limitations of a low-speed drive, RBCs remain beneficial due to their process efficiency. In RBCs, partial submersion and disc rotation (1–10 rpm) ensure continuous oxygenation, eliminating the need for an additional air diffusion system. Consequently, RBC energy consumption is relatively low, ranging around 0.02 – 0.05 kWh/m³ of treated wastewater [33]. In contrast, in conventional activated sludge (CAS) and membrane bioreactor (MBR) systems, the biomass is maintained in suspension. The specific energy consumption of CAS and MBR systems is 0.15-0.7 kWh/m³ and 0.5-3.0 kWh/m³, respectively [34][35][36][37], with aeration accounting for up to 80% [38][39]. Despite its performance limitations, the proposed system's low power consumption could be adapted to battery-based operation, solar power, or other alternative energy sources. For instance, in water pumping applications, solar-powered BLDCs can replace conventional AC induction pumps [40]. Also, sensor-controlled systems should be tested to simplify the drive assembly (e.g., by reducing the number of cascaded MGs) and improve energy efficiency. For example, the system can save energy by doing a quarter-turn at a time, allowing the drive system to de-energize between moves.

5) Limitations

While focusing on accessibility and serviceability for developing DEWATS, the maintenance and operation of bioremediation technologies remain challenging. On the one hand, the removal efficiency of RBCs has been evaluated for complex organic compounds, such as antibiotics and pharmaceuticals [41][42], but results are often limited to controlled laboratory conditions. On the other hand, biological processes in WWTPs are sensitive to environmental perturbations, including operational disturbances, thus requiring constant monitoring and control. While RBCs perform well for wastewater with a moderate pollutant load, this study did not test essential operational parameters, and the prototype's expected performance was inferred from the literature. In real-world applications, the oxygen transfer system, including air supply and exhaust, would be critical.

Additional challenges remain with respect to the mechanical drive, as material selection affects durability and reliable operation in harsh environmental conditions. For instance, the pipe adaptor for the in-runner BLDC and the magnetic gear housing should be non-corrosive and chemically resistant. 3D-printable and advanced materials, such as aluminum alloys, PVDF, and duplex steel, could be used for thin sections to minimize the air gap. Nevertheless, from an economic perspective, a straightforward, robust design should be preferred to promote reliable performance and to facilitate rapid, local maintenance when needed. The system architecture presented in this study favors modular units over simple scalability, enabling non-specialists to operate it and allowing components to be exchanged or repaired off-site.

V. Conclusion

This paper presented a novel prototype based on RBC, BLDC, and MG technologies, developed as a proof-of-concept for DEWATS. First, the BLDC's performance was acceptable even with a larger radial air gap. Second, the MG's torque capacity was sufficient for maintaining the system's rotation. Experimental results demonstrate the approach's feasibility, with future work aimed at optimization and scale-up. Main challenges have been identified. First, durability and performance in real-world settings depend on selecting high-performance materials for the drive assembly. Second, a plug-and-play approach should focus on pre-assembled units that can be rapidly connected and disconnected for a swap-and-go servicing model. Finally, a sensored BLDC design should also be considered, and the use of other MG configurations, including axial-flux and Halbach arrays, should be investigated.

Conflict of Interest

The author declares no conflict of interest.

Author Contributions

The author was solely responsible for all aspects of this work, including conceptualization, methodology, data collection, analysis, manuscript preparation, visualization, project administration, and funding acquisition.

Funding

The study was supported by the Macao Science and Technology Development Fund (Project 0037/2024/ITP2).

Acknowledgment

The author wishes to thank Saw Darwi Htoo and Choi Man Chon for their participation in preparing various components of the system, and Lei Chi Chon for his help in procuring the BLDC stator.

References

[1] J.-R. S. Ventura, J. U. Tulipan, A. Banawa, K. D. C. Umali, and J. A. L. Villanueva, "Advancements and challenges in decentralized wastewater treatment: A comprehensive review," *Desalination and Water Treatment*, vol. 320, p. 100830, Oct. 2024, doi: 10.1016/j.dwt.2024.100830.

[2] D. Kour *et al.*, "Microbe-mediated bioremediation: Current research and future challenges," *J App Biol biotech*, pp. 6–24, Jun. 2022, doi: 10.7324/JABB.2022.10s202.

[3] V. Pande, S. C. Pandey, D. Sati, V. Pande, and M. Samant, "Bioremediation: an emerging effective approach towards environment restoration," *Environmental Sustainability*, vol. 3, no. 1, pp. 91–103, Mar. 2020, doi: 10.1007/s42398-020-00099-w.

[4] A. Capodaglio, "Integrated, decentralized wastewater management for resource recovery in rural and peri-urban areas," *Resources*, vol. 6, no. 2, p. 22, Jun. 2017, doi: 10.3390/resources6020022.

[5] S. Hube and B. Wu, "Mitigation of emerging pollutants and pathogens in decentralized wastewater treatment processes: A review," *Science of The Total Environment*, vol. 779, p. 146545, Jul. 2021, doi: 10.1016/j.scitotenv.2021.146545.

[6] M. A. Mohameda, H. A. Fouad, and R. M. ElHefny, "Reviewing rotating biological contactor's different aspects for wastewater treatment with experiment," *Engineering Research Journal - Faculty*

of Engineering (Shoubra)*, vol. 51, no. 2, pp. 180–187, Apr. 2022, doi: 10.21608/erjsh.2022.239936.
[7] P. A. Kadu and Y. R. M. Rao, "A Review of rotating biological contactors system," *IJERA*, vol. 2, no. 5, pp. 2149–2153, 2012.
[8] A. G. Mizyed, "Review on application of rotating biological contactor in removal of various pollutants from effluent," *Technium BioChemMed*, vol. 2, no. 1, pp. 41–61, 2021.
[9] R. Ravi, K. Sarayu, S. Sandhya, and T. Swaminathan, "Rotating Biological Contactors," in *Air Pollution Prevention and Control*, 1st ed., C. Kennes and M. C. Veiga, Eds., Wiley, 2013, pp. 207–220. doi: 10.1002/9781118523360.ch9.
[10] S. Cortez, P. Teixeira, R. Oliveira, and M. Mota, "Rotating biological contactors: a review on main factors affecting performance," *Rev Environ Sci Biotechnol*, vol. 7, no. 2, pp. 155–172, Jun. 2008, doi: 10.1007/s11157-008-9127-x.
[11] D. Mba, "Mechanical evolution of the rotating biological contactor into the 21st century," *Proceedings of the Institution of Mechanical Engineers, Part E: Journal of Process Mechanical Engineering*, vol. 217, no. 3, pp. 189–219, Aug. 2003, doi: 10.1243/095440803322328863.
[12] W. G. Gilbert, J. F. Wheeler, and A. MacGregor, "Energy Usage of Rotating Biological Contactor Facilities," *Journal WPCF*, vol. 58, no. 1, pp. 47–51, 1986.
[13] D. Mba, R. H. Bannister, and G. E. Findlay, "Mechanical redesign of the rotating biological contactor," *Water Research*, vol. 33, no. 18, pp. 3679–3688, Dec. 1999, doi: 10.1016/S0043-1354(99)00086-X.
[14] B. Divakar, "A Review On Brushless Dc Motor Control Techniques," *Journal of Pharmaceutical Negative Results*, vol. 13, no. 7, pp. 6821–6828, 2022.
[15] D. Mohanraj *et al.*, "A review of BLDC motor: State of art, advanced control techniques, and applications," *IEEE Access*, vol. 10, pp. 54833–54869, 2022, doi: 10.1109/ACCESS.2022.3175011.
[16] A. V. Schagin and D. T. Nguyen, "Development of speed control system for BLDC motor with power factor correction," in *2020 IEEE Conference of Russian Young Researchers in Electrical and Electronic Engineering (EIConRus)*, St. Petersburg and Moscow, Russia: IEEE, Jan. 2020, pp. 2411–2414. doi: 10.1109/EIConRus49466.2020.9038981.
[17] R. Jauhar, N. Ismail, and N. Sartika, "Design of torque controller based on field-oriented control (FOC) method on BLDC motor," in *2022 16th International Conference on Telecommunication Systems, Services, and Applications (TSSA)*, Lombok, Indonesia: IEEE, Oct. 2022, pp. 1–5. doi: 10.1109/TSSA56819.2022.10063889.
[18] Y. Yang *et al.*, "REE eecovery from end-of-life NdFeB permanent magnet scrap: A critical review," *J. Sustain. Metall.*, vol. 3, no. 1, pp. 122–149, Mar. 2017, doi: 10.1007/s40831-016-0090-4.
[19] T. Kim, H.-W. Lee, and M. Ehsani, "Position sensorless brushless DC motor/generator drives: review and future trends," *IET Electr. Power Appl.*, vol. 1, no. 4, pp. 557–564, Jul. 2007, doi: 10.1049/iet-epa:20060358.
[20] P. Visconti and P. Primiceri, "An overview on state-of-art and future application fields of BLDC motors: design and characterization of a PC-interfaced driving and motion control system," *ARPN Journal of Engineering and Applied Sciences*, vol. 12, no. 17, pp. 4913–4926, 2017.
[21] S. Tabraiz, S. Haydar, and G. Hussain, "Evaluation of a cost-effective and energy-efficient disc material for rotating biological contactors (RBC), and performance evaluation under varying condition of RPM and submergence," *Desalination and Water Treatment*, vol. 57, no. 43, pp. 20493–20500, Sep. 2016, doi: 10.1080/19443994.2015.1113143.
[22] J. Szulżyk-Cieplak, A. Tarnogórska, and Z. Lenik, "Study on the influence of selected technological parameters of a rotating biological contactor on the degree of liquid aeration," *J. Ecol. Eng.*, vol. 19, no. 6, pp. 247–253, Nov. 2018, doi: 10.12911/22998993/92512.
[23] A. Al Faysal, S. Mohamed Haris, "Development of Magnetic Gears: A Review," *JKUKM*, vol. SI 1, no. 7, pp. 49–56, Nov. 2018, doi: 10.17576/jkukm-2018-si1(7)-06.
[24] P. Griffin and G. E. Findlay, "Process and engineering improvements to rotating biological contactor design," *Water Science and Technology*, vol. 41, no. 1, pp. 137–144, Jan. 2000, doi: 10.2166/wst.2000.0022.
[25] X. Yan, X. Liang, W. Ouyang, Z. Liu, B. Liu, and J. Lan, "A review of progress and applications of ship shaft-less rim-driven thrusters," *Ocean Engineering*, vol. 144, pp. 142–156, Nov. 2017, doi: 10.1016/j.oceaneng.2017.08.045.
[26] Texas Instruments Incorporated, *InstaSPIN-FOC^{TM} and InstaSPIN-MOTION^{TM}*. Dallas, TX, 2021.
[27] S. Z. Radosavljević, B. Ž. Stojanović, and A. D. Skulić, "Determination of power losses in worm gear reducer," *IOP Conf. Ser.: Mater. Sci. Eng.*, vol. 393, p. 012050, Aug. 2018, doi: 10.1088/1757-899X/393/1/012050.
[28] T. Kuphaldt and J. Haughery, *Applied industrial electricity: theory and application*. Iowa State University Digital Press, 2020. doi: 10.31274/isudp.2020.31.
[29] A. Fauzi, W. T. Handoyo, A. R. Hakim, and F. Hidayat, "Performance and energy consumption of paddle wheel aerator driven by brushless DC motor and AC motor: A preliminary study," *IOP Conf. Ser.: Earth Environ. Sci.*, vol. 934, no. 1, p. 012010, Nov. 2021, doi: 10.1088/1755-1315/934/1/012010.
[30] K. Atallah and D. Howe, "A novel high-performance magnetic gear," *IEEE Trans. Magn.*, vol. 37, no. 4, pp. 2844–2846, Jul. 2001, doi: 10.1109/20.951324.
[31] M. K. Jaison, K. H. Meharban, S. Shilpa, G. Swathi, and S. S. Jawahar, "Performance analysis of rotating biological contactor with polypropylene and wool media," *IJCIET*, vol. 8, no. 3, pp. 771–777, 2017.
[32] S. Waqas *et al.*, "A review of rotating biological contactors for wastewater treatment," *Water*, vol. 15, no. 10, p. 1913, May 2023, doi: 10.3390/w15101913.
[33] F. Hassard, J. Biddle, E. Cartmell, B. Jefferson, S. Tyrrel, and T. Stephenson, "Rotating biological contactors for wastewater treatment – A review," *Process Safety and Environmental Protection*, vol. 94, pp. 285–306, Mar. 2015, doi: 10.1016/j.psep.2014.07.003.
[34] U. Ghimire, G. Sarpong, and V. G. Gude, "Transitioning wastewater treatment plants toward circular economy and energy sustainability," *ACS Omega*, vol. 6, no. 18, pp. 11794–11803, May 2021, doi: 10.1021/acsomega.0c05827.
[35] P. Krzeminski, J. H. J. M. Van Der Graaf, and J. B. Van Lier, "Specific energy consumption of membrane bioreactor (MBR) for sewage treatment," *Water Science and Technology*, vol. 65, no. 2, pp. 380–392, Jan. 2012, doi: 10.2166/wst.2012.861.
[36] A. Siatou, A. Manali, and P. Gikas, "Energy consumption and internal distribution in activated sludge wastewater treatment plants of Greece," *Water*, vol. 12, no. 4, p. 1204, Apr. 2020, doi: 10.3390/w12041204.
[37] K. Yamashita, H. Itokawa, and T. Hashimoto, "Demonstration of energy-saving membrane bioreactor (MBR) systems," *Water Science and Technology*, vol. 79, no. 3, pp. 448–457, Feb. 2019, doi: 10.2166/wst.2019.068.
[38] B. Barillon, S. M. Ruel, C. Langlais, and V. Lazarova, "Energy efficiency in membrane bioreactors," *Water Science and Technology*, vol. 67, no. 12, pp. 2685–2691, Jun. 2013, doi: 10.2166/wst.2013.163.
[39] M. Muloiwa, M. O. Dinka, and S. Nyende-Byakika, "Modelling and optimization of energy consumption in the activated sludge biological aeration unit," *Water Practice and Technology*, vol. 18, no. 1, pp. 140–158, Jan. 2023, doi: 10.2166/wpt.2022.154.
[40] R. Nisha and K. Gnana Sheela, "Review of PV fed water pumping systems using BLDC Motor," *Materials Today: Proceedings*, vol. 24, pp. 1874–1881, 2020, doi: 10.1016/j.matpr.2020.03.612.
[41] N. Delgado, A. Navarro, D. Marino, G. A. Peñuela, and A. Ronco, "Removal of pharmaceuticals and personal care products from domestic wastewater using rotating biological contactors," *Int. J. Environ. Sci. Technol.*, vol. 16, no. 1, pp. 1–10, Jan. 2019, doi: 10.1007/s13762-018-1658-2.
[42] A. C. Del Álamo, M. I. Pariente, R. Molina, and F. Martínez, "Advanced bio-oxidation of fungal mixed cultures immobilized on rotating biological contactors for the removal of pharmaceutical micropollutants in a real hospital wastewater," *Journal of Hazardous Materials*, vol. 425, p. 128002, Mar. 2022, doi: 10.1016/j.jhazmat.2021.128002.